Metal accumulation by Alyssum serpyllifolium subsp. malacitanum Rivas Goday (Brassicaceae) across different petrographic entities in South-Iberian ultramafic massifs: plant-soil relationships and prospects for phytomining

Journal:	*International Journal of Phytoremediation*
Manuscript ID	Draft
Manuscript Type:	Original Article
Date Submitted by the Author:	n/a
Complete List of Authors:	Manteca-Bautista, David; University of Malaga Hidalgo Triana, Noelia; University of Malaga, Pérez-Latorre, Andrés ; University of Malaga Freitas, Helena; University of Coimbra
Keywords:	metal hyperaccumulator, bioaccumulation factor, inter-population variation

title page

Title

Metal accumulation by *Alyssum serpyllifolium* subsp. *malacitanum* Rivas Goday (Brassicaceae) across different petrographic entities in South-Iberian ultramafic massifs: plant-soil relationships and prospects for phytomining

David Manteca Bautista[a], Hidalgo-Triana, N[a]*, Andrés V. Pérez Latorre[a] and Helena Freitas[b]

[a]*Department of Botany and Plant Physiology, University of Malaga, Malaga, Spain;*
[b]*Department of Life Sciences, University of Coimbra, Coimbra, Spain;*

*corresponding author: nhidalgo@uma.es. University of Malaga. Department of Botany and Plant Physiology, Faculty of Science, University of Malaga, 29010. Malaga, Spain. Noelia Hidalgo-Triana: ORCID: https://orcid.org/0000-0002-5343-369X

Author information

- David Manteca Bautista. Malaga, Spain. ORCID: https://orcid.org/0000-0001-9489-5607. Department of Botany and Plant Physiology, Faculty of Science, University of Malaga, 29010. Malaga, Spain

- * Noelia Hidalgo Triana. Corresponding author: nhidalgo@uma.es. University of Malaga. Department of Botany and Plant Physiology, Faculty of Science, University of Malaga, 29010. Malaga, Spain. Noelia Hidalgo-Triana: ORCID: https://orcid.org/0000-0002-5343-369X. +34952131952.

- Andrés V. Pérez Latorre. University of Malaga. Department of Botany and Plant Physiology, Faculty of Science, University of Malaga, 29010. ORCID: https://orcid.org/0000-0002-9027-9927

- Helena Freitas. Centre for Functional Ecology - Science for People & the Planet. Department of Life Sciences. University of Coimbra. Portugal. ORCID http://orcid.org/0000-0002-1907-9615

Novelty statement

To date, studies of hyperaccumulation in plant tissues on ultramafic rocks have not considered the great diversity of petrographic entities in the world's outcrops. One of them is the one that we studied in Spain with more than eight petrographic entities and different soils.

Our hypothesis is that the different chemical compositions of the soils in ultramafic rocks significantly affect the hyperaccumulation of metals by specialised plants, which may have consequences for phytomining. For this purpose, individuals, populations and different soils have been tested and the results have been subjected to the corresponding statistical tests. The obtained knowledge reflects the different behaviour of the studied plant not only for the Ni: the obtained results for Sr and for Ba revealed interesting results for the hyperaccumulation in *Alyssum* of both metals.

ABSTRACT

In the ultramafic area of Spain, a high quantity of petrographic entities is present. Data on the variability between populations of hyperaccumulation are scarce. We investigated *Alyssum serpyllifolium* subsp. *malacitanum* for variation in eleven elements between populations growing in different ultramafic massifs across different petrographic entities (dunites, harzburgite-pyroxenic dunite, harzburgite-lherzolite, pyroxenite and serpentinites).

Samples of leaves and soils were collected from the ultramafic outcrops of Sierra Bermeja and Sierra de Mijas (Andalusia, Spain). Concentrations of Ni, Fe, Mg, Si, Cr, Co, Sr, Mn, Cu, Zn and Ba and the Bioaccumulation factors (BAF) were determined.

Although analysis of variance of data for each element revealed considerable variation in the soil chemistry (for Fe, Mg, Sr and Ba) across different petrographic entities, population-level variation with regard to the hyperaccumulation in the leaves was not detected. BAF values greater than one were obtained for Sr and Ni depending on the petrographic entities. The correlation detected between the concentration of Ni in the leaves and its concentration in the soil is relevant.

The population-level variation obtained in the BAF for Sr and Ni provide comprehensive information on the natural variation of hyperaccumulation. The BAF obtained for Ba is an important result for phytomining.

KEYWORDS: Serpentinophyte; metal hyperaccumulator; bioaccumulation factor; inter-population variation; Iberian Peninsula; Sierra Bermeja; Sierra de Mijas.

Metal accumulation by *Alyssum serpyllifolium* subsp. *malacitanum* Rivas Goday (Brassicaceae) across different petrographic entities in South-Iberian ultramafic massifs: plant-soil relationships and prospects for phytomining

ABSTRACT

In the ultramafic area of Spain, a high quantity of petrographic entities is present. Data on the variability between populations of hyperaccumulation are scarce. We investigated *Alyssum serpyllifolium* subsp. *malacitanum* for variation in eleven elements between populations growing in different ultramafic massifs across different petrographic entities (dunites, harzburgite-pyroxenic dunite, harzburgite-lherzolite, pyroxenite and serpentinites).

Samples of leaves and soils were collected from the ultramafic outcrops of Sierra Bermeja and Sierra de Mijas (Andalusia, Spain). Concentrations of Ni, Fe, Mg, Si, Cr, Co, Sr, Mn, Cu, Zn and Ba and the Bioaccumulation factors (BAF) were determined.

Although analysis of variance of data for each element revealed considerable variation in the soil chemistry (for Fe, Mg, Sr and Ba) across different petrographic entities, population-level variation with regard to the hyperaccumulation in the leaves was not detected. BAF values greater than one were obtained for Sr and Ni depending on the petrographic entities. The correlation detected between the concentration of Ni in the leaves and its concentration in the soil is relevant.

The population-level variation obtained in the BAF for Sr and Ni provide comprehensive information on the natural variation of hyperaccumulation. The BAF obtained for Ba is an important result for phytomining.

KEYWORDS: Serpentinophyte; metal hyperaccumulator; bioaccumulation factor; inter-population variation; Iberian Peninsula; Sierra Bermeja; Sierra de Mijas.

Introduction

Hyperaccumulation of metals (and metalloids) by plants has been studied extensively over the past decades although it is a rare phenomenon, known presently in only approximately 0.2% of angiosperms (Krämer 2010). Hyperaccumulators are plants that absorb and store in their shoots exceptionally high concentrations of elements typically found in trace quantities in soils (van der Ent *et al.* 2013).

Heavy metals are mostly transition metals that can be both essential, such as Fe, Zn, Mn, Cu, Ni, Mo and Co and non-essential (Marschner 2016); for example, chromium (Cr), cadmium (Cd), mercury (Hg) and lead (Pb). In the case of some soils in which the local bedrocks are serpentines, gypsums and dolomites, high concentrations of metals may be found in the rhizosphere solution, as ions or as part of complexes with organic or inorganic compounds (Kazakou *et al.* 2008). Therefore, these soils exert a high selective pressure, leading to the assembly of a characteristic flora (Rajakaruna 2004) composed mainly of obligate metallophytes or hyperaccumulators (Kazakou *et al.* 2008) with different efficiencies to uptake or exclude a variety of metals (Verbruggen *et al.* 2009; Morais *et al.* 2015); some of them originating edaphisms and endemisms (Mota *et al.* 2017).

Though generally soils developed over ultramafic rocks are characterized by high contents of Cr, Mg, Ni, Fe, Mn and Co, low levels of nutrients, and a low quotient of Ca/Mg, the different mineralogical and lithological composition of the ultramafic units of the massifs can generate different elemental concentrations of metals in soils (Morais *et al.* 2015).

Nickel accumulation is the most frequent response in serpentine soils derived from weathering of ultramafic rocks (van der Ent *et al.* 2019). For hyperaccumulation, most researchers have adopted standard threshold criteria. The first example for hyperaccumulation for Ni in plant dry matter is 1000 $mg \cdot kg^{-1}$ (Krämer 2010; Sheoran *et al.* 2010; van der Ent *et al.* 2013), equivalent to 1.0 $g \cdot kg^{-1}$ or 0.1% (Brooks *et al.* 1981). Subsequently, hyperaccumulation criteria have been proposed for other metals, sometimes at lower or higher concentrations depending on the abundance of the respective elements in nature (van der Ent *et al.* 2013). This capacity for metal accumulation manifested by some plant taxa implied possible technological applications (Prasad and Freitas 1999).

In the Mediterranean basin and South Western Asia, a remarkable diversity of Ni hyperaccumulating taxa occurs in the Alysseae tribe of the Brassicaceae family (Rivas-Goday 1973). *Alyssum serpyllifolium* Desf. (Brassicaceae) is widespread on limestone as well as serpentine soils of Iberian Peninsula and southern France (de la Fuente *et al.* 2007; Morais *et al.* 2015). The serpentine populations have often been treated as distinct species or subspecies: there are two well-known Ni hyperaccumulators subspecies (Rivas-Goday 1973; Brooks and Radford 1978; Brooks *et al.* 1979, 1981; Menezes de Sequeira and Pinto da Silva 1992; Asensi *et al.* 2004; de la Fuente *et al.* 2007) that grow naturally on ultramafic soils of the Iberian Peninsula: subsp. *lusitanicum* Dudley and P. Silva in Portugal and subsp. *malacitanum* Rivas Goday in Spain (Freitas *et al.* 2004; Blanca *et al.* 2011; Pérez Latorre *et al.* 2013).

A. serpyllifolium subsp. *malacitanum* (=*Odontarrhena serpyllifolia* (Desf.) Jord. & Fourr (Španiel *et al.* 2015) is representative of the ultramafic chamaephytic vegetation of Southern Iberian Peninsula (Malaga), one of the bigger ultramafic area in the Western Mediterranean, composed by the outcrop of Sierra Bermeja and other seven small outcrops with ecological differences due mainly to the petrographic entities of the peridotites (whit a wide range of variations in terms of mineral chemistry and mineral assemblage), climate and geomorphology (Gómez-Zotano *et al.* 2015; Morishita *et al.* 2015).

Although Brooks *et al.* (1981), Asensi *et al.* (2004), Rufo *et al.* (2005) and de la Fuente *et al.* (2007) established that the *A. serpyllifolium* subsp. *malacitanum* population of Sierra Bermeja reaches high Ni accumulation levels, inter-population variability across the different South Iberian outcrops has not been studied yet, obviating the detected variability in the capacity for accumulation of Ni, Zn and Cd in various populations of other plants (Sterckeman *et al.* 2017; Mišljenović *et al.* 2019). The complexity and abundance of those mechanisms result from the adaptive responses evolved during millions of years inhabiting different types of substrates (Shabala 2013; van der Ent *et al.* 2015). Assunção *et al.* (2003) and Brady *et al.* (2005) emphasized that plant adaptation to different soil types is evidence of the strong natural selection imposed by ecological discontinuities like the soil metal compositions at the population sites and Sterckeman *et al.* (2017) detected this variability in various populations of other Brassicaceae species.

The present study has the following objectives:

(1) to know quantitatively which elements characterize each soil in relation with parental petrographic entity (dunites, harzburgites-pyroxenic dunite, harzburgite-lherzolite, pyroxenites, serpentinites) according to the existent National Geological Map (MAGNA50) which was georeferenced for this work; (2) to verify variability in Ni and

other metals (Zn, Fe, Mg, Si, Cr, Co, Sr, Mn, Cu and Ba) accumulation by *A. serpyllifolium* subsp. *malacitanum* at different locations of ultramafic areas of South of Spain (Sierra Bermeja and Sierra de Mijas massifs), studying inter-populations variability in two outcrops that cover all types of peridotite petrographic entities of the southern Iberia. Additionally, it is our objective to obtain the bioaccumulation factor for each metal, and (3) to investigate the relationship between the metal concentration in the soil (total fraction) and the concentration in the plant.

The serpentine outcrops of the southern Iberian Peninsula support our hypothesis that the different petrographic entities present in different massifs should present different metal concentrations generating different responses of hyperaccumulation.

Materials and methods

Location, geology, climate, soils and vegetation

The study areas are located in the South of Spain, in a Mediterranean serpentine area. The ultramafic rocks of this territory are represented in different massifs, two of them studied in this work (Fig. S1) namely the Sierra Bermeja (Estepona, Malaga) massif and the Sierra de Mijas massif (Mijas, Malaga).

Geologically, according to the MAGNA50 (at 1:50000 scale; Instituto Geologico y Minero de España 1978; Fig. S1), these Bermeja and Mijas massifs are composed of different ultramafic petrographic entities: several petrographic entities in the Sierra Bermeja massif (Fig. S2A) and only serpentinites in the Sierra de Mijas massif (Fig. S2B, Table S1).

MAGNA50 has been georeferenced and converted in a shape file for this work to facilitate the recognition of the geological substrate at each sampling site (Fig. S2 A, B).

The bioclimatic characterization of both areas (Table S1) corresponds to the Mediterranean macrobioclimate, an extensive subhumid-humid thermomediterranean to dry mesomediterranean level in the Sierra Bermeja massif and thermomediterranean subhumid for Sierra de Mijas (Rivas Martínez *et al.* 2002). The dominant soil types in both massifs are entisols (Table S1) according to USDA classification (Rowell 2014). According to Pérez Latorre *et al.* (1998, 2013), the main pre-forest vegetation of Sierra Bermeja massif is characterised by scrublands of *Halimio atripicifolii-Digitaletum* *laciniatae* (Table S1). The dominant vegetation of Sierra de Mijas massif is a graminoid perennial pasture of *Scorzonero baeticae-Macrochloetum tenacissimae* (Gálvez-Villamuela *et al.* 2021; Table S1).

The Ni hyperaccumulator *A. serpyllifolium* subsp. *malacitanum* is present in almost all the serpentine vegetation types and grows in the majority of serpentine massifs (Asensi *et al.* 2004; Blanca et al 2011; Perez Latorre *et al.* 2013).

Field sampling and sample preparation

Samples of soils and *A. serpyllifolium* subsp. *malacitanum* leaves were collected from five random sites with different petrographic entities in the study areas (Sierra Bermeja and Mijas massifs; Fig. S1; Fig. S2 A, B), including four sites in the massif of Sierra Bermeja (Bd, Bh, Bl, Bp) and one site in the massif of Sierra de Mijas (Ms).

At each location, three random partial soil samples weighing 0.5 kg each were collected from a 0-20 cm depth (Morais *et al.* 2015), near to *A. serpyllifolium* subsp. *malacitanum*. And leaves of three individuals of *A. serpyllifolium* subsp. *malacitanum* were randomly collected for analysis with a minimal distance between plant individuals was 5 m and the minimal straight-line distance between the sampling points was 2.38 km following Mišljenović *et al.* (2019). In the laboratory, the soil samples were oven-dried at a constant temperature of 40 ºC and were then manually sieved with 2, 0.5 and 0.1 sieves consecutively to obtain fine powder.

Analytical procedures

The determination of total element content (Ba, Cr, Co, Cu, Fe, Mg, Mn, Ni, Si, Sr and Zn) in the soil samples was performed using two different instrumental techniques: ICP-AES (Fe, Mg and Si) and ICP-MS (for the rest of elements). Soil samples were dried in a stove at 150 ºC. 0.1 g of each sample was taken for analysis. Each sample was weighed into a digester tube using an analytical balance. Subsequently, an acid digestion was carried out using a microwave pressure digester oven with a 15-position rotor UltraWAVE model (Milestone®□) at 240 ºC and 40 bar. 1 mL of HNO_3 (65%), 3 mL of HCl (37%), 2 mL of HF (49%) and 10 mL of H_3BO_3 (5%) were added to the samples. Once the digestion was completed, the samples were made up to a final volume of 25 mL with quality 1 deionized water (18.2 MΩ·cm).

The analytical processes for the leaves involved freezing to -80 ºC and subsequently lyophilized during 48 h employing a LyoQuest (Telstar®□) freeze dryer. Then, dry samples were milled with agate mortar. 0.25 g of each sample were taken for analysis. Each sample was weighed into a digester tube using an analytical balance. Subsequently, an acid digestion was carried out using a microwave pressure digester oven with a 15-position rotor UltraWAVE model (Milestone®□) at 240 ºC and 40 bar. 3 mL of HNO3 (65%), 1 mL of HCl (37%), 0.5 mL of HF (49%) and 2.5 mL of H_3BO_3 (5%) were added to the samples. Once the digestion was completed, the samples were made up to a final volume of 25 mL with quality 1 deionized water (18.2 MΩ·cm). Metal concentration was measured using two different instrumental techniques.

Data were collected in triplicate, making a total of 15 plant samples and 15 soil samples (3 samples per site). All the samples were processed in the SCAI-UMA technical services of the University of Malaga.

Data processing

The normality for elemental concentration in the leaves and soils was evaluated using the Shapiro-Wilk test. Variables studied turned out not to be normal. The differences in the elemental concentration of metals in the leaves and in the soil samples among the petrographic entities of the different ultramafic massifs studies (intra-population variation) were performed using the Kruskal-Wallis test, pairwise comparisons were performed by Dunn's procedure followed by Bonferroni corrections. The relationships between sites with respect to chemical characteristics of each petrographic entity were determined using the principal components analysis (PCA). Furthermore, the relationships between elemental concentration in the leaves and in the soils were analysed by Spearman rank order correlations. For significant correlations, the regression coefficient was determined. Finally, bioaccumulation factor (BAF) was calculated as a ratio between the concentrations of elements in the leaves and in the respective soils following Pavlova and Karadjova (2013).

All the statistical procedures were carried out with R software.

Results

Soil elemental concentration and chemical soil analyses

Results of soil samples analyses are shown in Table S2. Some chemical soil parameters varied widely across different sampling sites. Mean concentrations of Ni varied from 2571.00 mg·kg^{-1} on Bd to 3593.33 mg·kg^{-1} on Bh showing a reduced CV (<18%). The soil samples collected on Ms showed the highest mean concentrations for Fe showing a trend as follow: Ms > Bh > Bl > Bp > Bd (155006.67 mg·kg^{-1}; Fig. 1A); Co (261.98 mg·kg^{-1}), Sr (27.69 mg·kg^{-1}; Fig. 1C) following a trend as follow: Ms > Bl > Bh > Bd > Bp; Mn (2428.67 mg·kg^{-1}); Zn (143.89 mg·kg^{-1}) and Ba with the same sequence as the concentration of Sr and a mean concentration of 85.87 mg·kg^{-1} (Fig. 1D); while soil samples collected on Bd showed the highest mean concentrations for Mg (140466.67 mg·kg^{-1}; Fig. 1B) with a trend as follow Bd > Bh > Bl > Bp > Ms and Cu (64.47 mg·kg^{-1}), the soil samples collected on Bh reached the highest value for Cr (8089 mg·kg^{-1}) and for Ni (3593.33 mg·kg-1). Finally, the soil samples collected on Bp reached the highest values for Si (162633.33 mg·kg^{-1}; Table S2). According to Kruskal-Wallis test, there was a significant difference between the petrographic entities of Fe, Mg, Sr and Ba (Table 1). The Bonferroni correction for multiple comparisons indicated that the concentration of Fe and Mg were different between Bd and Ms (0.01 and 0.02 respectively) and for the concentration of Sr and Ba the group of Ms and Bp (0.01 and 0.01 respectively); resulting Ms as different of the rest.

The results of the PCA (Fig. 2; Table S3) showed a certain separation between different petrographic sites. The first two axes supported 98% of the variance. The first axis represents 84% of the accumulated variance and it was positively correlated with concentrations of Fe (Ms). The second axis represents 14% of the accumulated variance and it was positively correlated with concentration of Si (Bp) and negatively with Mg.

Plant analyses

The results of the leaf samples analyses are presented in Table S2. Nickel concentrations in the leaves varied greatly (CV>30%; N=15) and all ultramafic populations were Ni hyperaccumulating. The highest mean concentration of Ni, over 11000 mg·kg^{-1}, was recorded in the leaves collected on Bl while the lowest, 6422.33 mg·kg^{-1}, was recorded in the leaves collected on Ms.

The concentrations of Fe in the leaves were highly variable (CV>50%), recording values around 1000 mg·kg^{-1} on Bl. Concentrations of Mg were not highly variable (CV<20%). The highest concentration of Cr in the leaves was found in the sample from Bl (37.18 mg kg^{-1}), as well as the very high CV in all leaf samples (CV>70%). Concentrations of Co showed a CV<35%, reaching concentration values between 35-48 mg·kg^{-1} across all the populations. Concentrations of Sr and Mn in the leaves showed a CV>20%, showing a mean value around 100 mg·kg^{-1}. The recorded concentrations of Cu in the leaves were values lower than 4 mg·kg^{-1} in all the studied leaves. Concentrations of Zn in the leaves were highly variable, with a low mean value (21.70 mg·kg^{-1}). Concentrations of Ba were highly variable (CV>40%) with a mean value of 16.53 mg·kg^{-1}. The leaf samples collected on Bd showed also the highest mean concentrations for Si, Sr and Ba, while leaf samples showed the highest mean concentrations for Co on Bh, Fe, Ni and Cr on Bl and Mn, Cu and Zn on Bp (Table S2).

The concentrations of Fe in the leaves were positively correlated with those of Si, Cr, Mn and Cu (ρ = 0.75; ρ = 0.85; ρ = 0.56; ρ = 0.60, respectively), the concentrations of Mg were positively correlated with those of Si, Mn and Cu (ρ = 0.75; ρ = 0.71; ρ = 0.56, respectively) and the concentrations of Si were positively correlated with Cr, Mn and Cu (ρ = 0.53; ρ = 0.85; ρ = 0.76, respectively; Table S4).

Spearman rank order correlations showed that the only parameter that presented a correlation between its concentration in the soil and in the leaves was the concentration of Ni (ρ = 0.544, p = 0.036; Table S5). That correlation between the concentration of Ni in leaves and the concentration of Ni in the soil was positive (R^2 = 0.3; Fig. 3).

The correlations between measured elemental concentrations in the leaves and their soils were variables depending on the elements (Table S5). The concentration of Fe in the soil correlated with the concentration of Mg (ρ = -0.63, p = 0.01), Si (ρ = -0.66, p = 0.01) and Cu (ρ = -0.72, p = 0.00) in the leaves; the concentration of Fe in the leaves correlated with the concentration of Cu in the soil (ρ = 0.58, p = 0.02); the concentration of Si in the soil correlated with the concentration of Cu (ρ = 0.532, p = 0.04) and Zn in the leaves (ρ =0.621, p = 0.01); the concentration of Ni in the soil correlated with the concentration of Co in the leaves (ρ =0.68, p = 0.00); the concentration of Cr in the soil correlated with the concentration of Cu in the leaves ($\rho = -0.59$, $p = 0.02$); the concentration of Co in the soil correlated with the concentration of Cu in the leaves ($\rho = -0.67$, $p = 0.01$); and finally, the concentration of Sr in the soil correlated with the concentration of Cu in the leaves ($\rho = -0.53$, $p = 0.04$).

Concentration in the leaves across the analysed populations

No statistically significant difference in concentrations of analysed metals in the leaves of the plant analysed between the samples from the different populations (different petrographic entities) according to Kruskal-Wallis test), although significant differences were shown in the soils between the populations (Table 1).

Bioaccumulation

Bioaccumulation factors (BAF) of different studied parameters across the studied petrographic units (populations) are presented in the Table 2. Values of BAF for Sr and Ni were found >1. The BAF for Ni showed a bioaccumulation trend as follows: Bl > Bp > Bd > Bh > Ms. In the case of BAF for Sr, the bioaccumulation trend was as follows: Bp > Bd > Bh > Bl > Ms. For the rest of the elements, BAF values were <1. Is worth mentioning that the values reached for Ba were close to one in Bd and Bp soils.

Discussion

Soil elemental composition

The concentration of metals in the studied soils was in agreement with observations reported by other authors for serpentine soils from other serpentine regions (Ghaderian *et al.* 2007; Bani *et al.* 2013; Morais *et al.* 2015; Álvarez-López *et al.* 2016; Romero-Freire *et al.* 2018; Mišljenović *et al.* 2019;). In our study, the concentration of Fe, Mg, Sr and Ba varied widely across the studied petrographic entities but the concentration of the rest of the analyzed metals did not show significant variation. In contrast, Romero-Freire *et al.* (2018) in their study on the Sierra Palmitera (which is allocated in Sierra Bermeja), did not detect significant differences in metals concentration among soils collected on the petrographic entities of harzburgites, lherzolites and serpentinites. The high concentration of Fe, Sr and Ba characterized serpentinite substrates (Ms) and the concentration of Mg characterized Bh. The detected differences of these metals across the studied petrographic entities may be explained by several factors, such as degree of serpentinization, content of organic matter, physicochemical characteristics of soils and other micro-edaphic factors (Mišljenović *et al.* 2019). Hattori and Guillot (2003) indicated that during the serpentinization process a Sr enrichment occurs, which explains the highest concentration of Sr detected by our study in the soils of the Ms massif. Sr is considered as a radionuclide that can affect life (Gupta and Walther 2018). For these reasons, phytomining activities with Fe and Sr hyperaccumulators could be implemented in Sierra de Mijas to prospect new phytomining knowledge (Rodríguez *et al.* 2005; Li *et al.* 2011).

Our soil samples collected on Bp showed the highest concentrations of Si. This is consistent with the fact that pyroxenite contains less olivine mineral than the rest of ultramafic rocks (Oliveras and Galán 2006). The soil samples collected on Bd showed the highest concentration of Mg which is consistent with the fact that the principal mineral component of dunites is olivine (Pons *et al.* 2000).

Although Díez Lázaro *et al.* (2006), Vithanage *et al.* (2014) and Morais *et al.* (2015) showed that nickel was the most bioavailable metal in all serpentine studies sites, our results did not show differences in the concentration of nickel across the soils of the studied petrographic entities. Although bioavailability was not studied in our study, the concentration of Ni was similar across the studied petrographic entities. The soil samples collected on Bh, Bl and Ms massifs showed the highest concentration of Ni in our study which were higher in comparison with other studies on different ultramafic soils (Ghaderian *et al.* 2007; Bani *et al.* 2013; Morais *et al.* 2015; Álvarez-López *et al.* 2016; Romero-Freire *et al.* 2018; Mišljenović *et al.* 2019).

Leaf elemental composition relationship with soil elemental composition

Although differences were detected in the concentration of Fe, Mg, Sr and Ba across the petrographic entities of the studied soils, no significant difference in concentrations of any metal in the leaves was detected. The concentration of Ba did not show correlation between the concentration in the leaves and in the soils but the concentration of Fe in the soil was negatively correlated with the concentration of Si, Cu and Mg in the leaves, which is consistent with the lowest hyperaccumulation reached on the Ms soils of Sierra de Mijas massif. The presence of Fe oxides could explain this effect observed in the hyperaccumulation (Morais *et al.* 2015).

Although the capacity for hyperaccumulation of Ni by *A. serpyllifolium* subsp. *malacitanum* was already demonstrated in the scientific literature, our study has proved that it maintains its ability as Ni hyperaccumulator regardless of the petrographic entity it grows on: the concentration of Ni in the leaves far exceeded the limit of 1000 mg·kg^{-1} considered by van der Ent *et al.* (2013). The hyperaccumulation obtained in the leaves collected from the population of Ms massifs reached the lowest hyperaccumulation while the soil samples collected in the Ms massifs showed the second higher content in Ni but the higher concentration in Fe and the generation of Fe oxides could be the explanation as it has been pointed out previously. The hyperaccumulation of Ni detected by Álvarez-López *et al.* (2016) from leaves samples collected in Sierra Bermeja (9527 mg·kg^{-1}) has been surpassed by our leaves collected on Bh with 10-fold variation (11324 mg·kg^{-1}).

However, it was noteworthy the positive correlations that Ni showed between the concentration in the leaves samples and in the soil samples which is in accordance with the results obtained by Brooks (1983) and Pollard *et al.* (2021) in hydroponic media. Nevertheless, Morais *et al.* (2015) did not observe this correlation (both in shoots and roots). Our positive correlation across the petrographic entities has confirmed that the hyperaccumulation depends on the Ni concentration in the soil and Ni in the soil was also positively correlated with the concentration of Co in the leaves which agrees with the results obtained by Keeling *et al.* (2003) and Rue *et al.* (2020), where the increase in the concentration of Ni in the soil promoted the uptake of Co in *Berkheya coddii*. In addition, the ability of Co to inhibit the uptake of Ni cited by Keeling *et al.* (2003) was also observed in our study, since the soil samples collected in the petrographic entity with the highest concentration of Co (261.98 mg·kg^{-1} on Ms) matches the leaf sample with the lowest concentration of Ni (6422.33 mg·kg^{-1} on Ms) collected in the same petrographic entity.

The leaf samples collected in Bd showed the highest concentration of Mg in this study. This is consistent with the fact that soil samples from Bd showed the highest concentration of this element and coincident with the results obtained by Pollard *et al.* (2021). In addition, differences were significant between soil samples from different petrographic units for the concentration of Mg. Despite this, Mg in the leaves only showed significant correlation with the concentration of Fe in the soil. It would be relevant to consider the concentration of bioavailable Mg in the soil.

With regard to the hyperaccumulation of Ba, the maximum concentration obtained in this study for leaf samples was 35.38 mg·kg^{-1}. There is no threshold established to consider a plant as a Ba hyperaccumulator, probably due to the few reports on barium accumulation in plants (Kowalska *et al.* 2012). However, there are studies which show plants with concentrations of Ba much higher than in our study (Li *et al.* 2011; Kowalska *et al.* 2012). In all probability, the threshold to consider a plant as Ba hyperaccumulator is higher than the concentration of Ba found in our study. This element could be considered in future hyperaccumulator studies.

Regarding Cr, Co, Cu, Zn and Mn elements, their concentrations in leaf samples in this study do not exceed the threshold set for them (Cr, Co, Cu: 300 mg·kg^{-1}, Zn: 3000 mg·kg^{-1}, Mn: 10000 mg·kg^{-1}; van der Ent *et al.* 2013) and there is no evidence that *A. serpyllifolium* subsp. *malacitanum* accumulates these elements in other studies. For the Fe element, there is no threshold by which to consider a plant as Fe hyperaccumulator. There are plants that can accumulate more than 10000 mg·kg^{-1} of Fe (Rodríguez *et al.* 2005), whereas in this study the concentration of Fe in leaf samples did not reach 1000 mg·kg^{-1}, in all probability *A. serpyllifolium* subsp. *malacitanum* cannot be considered as a Fe hyperaccumulator.

Bioaccumulation factor

A. serpyllifolium subsp. *malacitanum* only showed BAF >1 for Ni and Sr, and relatively close to 1 for Ba; the latter two bioaccumulation factors were detected in this study. These results suggest that this species is a useful tool for phytoremediation activities in polluted soils with these elements. In addition, this species showed a similar trend for BAF of Ni, Sr, Zn and Ba varying according to the petrographic entity indicating that the petrographic entity influences the accumulation of these elements. Due to this possible influence of the petrographic unit on the accumulation of some elements by plants, the importance of considering the mineralogical composition of the bedrock in hyperaccumulators studies should be highlighted, since usually most studies in this field do not consider this factor.

Despite the high BAF values of Sr obtained in our study, few studies include this element (Li *et al.* 2011; Wang *et al.* 2018). To consider Sr in future studies could be interesting due to Sr when is incorporated by plants, enters the food chain and causes serious threat to human health and the environment (Burger and Lichtscheidl 2019).

Conclusions

In the present study, high variability of Fe, Mg, Sr and Ba concentrations in soil across the different petrographic entities of the studied massifs has been detected showing that there are differences between the soils of the studied petrographic entities. The greatest differences have been detected in the serpentininte soil of Sierra de Mijas massif. Serpentinites are metamorphic rocks and the rest of the studied petrographic entities are igneous rocks.

Despite these differences detected in the soil, *A. serpyllifolium* subsp. *malacitanum* showed the same hyperaccumulation behaviour across the petrographic entities, maintaining its ability as Ni hyperaccumulator regardless of the petrographic unit. However, the only positive correlation detected between the concentration of Ni in the leaf samples and in the soil samples has confirmed an increase in the variability of the Ni hyperaccumulation depending on the concentration in the soil. In addition, the variation of bioaccumulation factor for Ni was related to the petrographic unit; higher for samples taken on harzburgite-lherzolite substrate and lower for samples taken on serpentinite substrates, which is an important result for prospect new phytomining activities.

The obtained BAF for Sr and for Ba revealed interesting results for the hyperaccumulation in plants of both metals. Finally, the ability to withstand different metal concentrations in different populations and petrographic units of ultramafic rocks make this species adaptable to different serpentine ecological habitats.

Funding

This work was supported by the Spanish Project “Cartografía de la Vegetación 806/03.2434” and the Master course “Biological diversity and Environment” of the University of Malaga (Spain) have partially financed this study.

The authors thanks to SCAI-UMA services for their help in the sampling and processing of leaves and soils.

Disclosure statement

No potential conflict of interest was reported by the authors.

Data availability statement

The data supporting the obtained results has been included in the manuscript.

References

Álvarez-López V, Prieto-Fernández Á, Cabello-Conejo M, Kidd P. 2016. Organic amendments for improving biomass production and metal yield of Ni-hyperaccumulating plants. Sci Total Environ. 548:370-379. doi:10.1016/j.scitotenv.2015.12.147.

Asensi A, Rodríguez N, Díez-Garretas B, Amils R. 2004. Nickel hyperaccumulation of some subspecies of *Alyssum serpyllifolium* (Brassicaceae) from ultramafic soils on the Iberian Peninsula. In: Boyd RS, Baker AJM, Proctor J, editors. Ultramafic rocks: their soils, vegetation and fauna. Proceedings of the Fourth International Conference on Serpentine Ecology; 2003 Apr 21-26. St Albans (UK): Science Reviews. p. 263-265.

Assunção A, Bookum W, Nelissen H, Vooijs R, Schat H, Ernst W. 2003. Differential metal-specific tolerance and accumulation patterns among *Thlaspi caerulescens* populations originating from different soil types. New Phytol. 159(2):411-419. doi:10.1046/j.1469-8137.2003.00819.x.

Bani A, Imeri A, Echevarria G, Pavlova D, Reeves R, Morel J, Sulçe S. 2013. Nickel hyperaccumulation in the serpentine flora of Albania. Fresenius Environ Bull. 22(6):1792-1801.

Blanca G, Cabezudo B, Cueto M, Salazar C, Morales C. 2011. Flora vascular de Andalucía Oriental [Vascular flora of Eastern Andalusia]. Sevilla (SP): Consejería de Medio Ambiente, Junta de Andalucía.

Brady K, Kruckeberg A, Bradshaw Jr H. 2005. Evolutionary ecology of plant adaptation to serpentine soils. Annu Rev Ecol Evol Syst. 36:243-266. doi:10.1146/annurev.ecolsys.35.021103.105730.

Brooks R. 1983. Biological methods of prospecting for minerals. New York (US): Wiley.

Brooks R, Morrison R, Reeves R, Dudley T, Akman Y. 1979. Hyperaccumulation of nickel by *Alyssum linnaeus* (Cruciferae). Proc R Soc Lond B Biol Sci. 203:387-403. doi:10.1098/rspb.1979.0005.

Brooks R, Radford C. 1978. Nickel accumulation by European species of the genus *Alyssum*. Proc R Soc Lond B Biol Sci. 200:217-224. doi:10.1098/rspb.1978.0016.

Brooks R, Shaw S, Asensi A. 1981. Some observations on the ecology, metal uptake and nickel tolerance of *Alyssum serpyllifolium* subspecies from the Iberian Peninsula. Vegetatio. 45:183-188. doi:10.1007/BF00054673.

Burger A, Lichtscheidl I. 2019. Strontium in the environment: review about reactions of plants towards stable and radioactive strontium isotopes. Sci Total Environ. 653:1458-1512. doi:10.1016/j.scitotenv.2018.10.312.

de la Fuente V, Rodríguez N, Díez-Garretas B, Rufo L, Asensi A, Amils R. 2007. Nickel distribution in the hyperaccumulator *Alyssum serpyllifolium* Desf. spp. from the Iberian Peninsula. Plant Biosyst. 142(2):170-180. doi:10.1080/11263500701401422.

Díez Lázaro J, Kidd PS, Monterroso Martínez C. 2006. A phytogeochemical study of the Trás-os-Montes region (NE Portugal): possible species for plant-based soil remediation technologies. Sci Total Environ. 354:265-277. doi:10.1016/j.scitotenv.2005.01.001.

Freitas H, Prasad MNV, Pratas J. 2004. Analysis of serpentinophytes from north-east of Portugal for trace metal accumulation-relevance to the management of mine environment. Chemosphere. 54(11):1625-1642. ISSN 0045-6535. doi:10.1016/j.chemosphere.2003.09.045.

Gálvez-Villamuela E, Hidalgo-Triana N, Pérez Latorre AV. 2021. Serpentine plant diversity and vegetation in a mediterranean area (Sierra de Mijas, Southern Iberian Peninsula, Spain). Ann di Bot. 11:135-154. doi:10.13133/2239-3129/17015.

Ghaderian S, Mohtadi A, Rahiminejad R, Baker A. 2007. Nickel and other metal uptake and accumulation by species of *Alyssum* (Brassicaceae) from the ultramafics of Iran. Environ Pollut. 145:293-298. doi:10.1016/j.envpol.2006.03.016.

Gómez-Zotano J, Roman-Requena F, Thorne J. 2015. Attributes and roadblocks: a conservation assessment and policy review of the Sierra Bermeja, a mediterranean serpentine landscape. Nat Areas J. 35(2):328-343. doi:10.3375/043.035.0215.

Gupta D, Walther C. 2018. Behaviour of strontium in plants and the environment. Cham (GE): Springer.

Hattori K, Guillot S. 2003. Volcanic fronts as a consequence of serpentinite dehydratation in the fore-arc mantle wedge. Geol Soc Am Bull. 31:525-528.

Instituto Geológico y Minero de España MAGNA 50. 1978. Mapa Geológico de España a escala 1:50.000 (2ª Serie). Madrid (SP): Ministerio de Ciencia e Innovación;

[accessed 2020 Jun 28]. http://info.igme.es/cartografiadigital/geologica/Magna50.aspx.

Kazakou E, Dimitrakopoulos P, Baker A, Reeves R, Troumbis A. 2008. Hypotheses, mechanisms and trade-offs of tolerance and adaptation to serpentine soils: from species to ecosystem level. Biol Rev. 83(4):495-508. doi:10.1111/j.1469-185X.2008.00051.x.

Keeling SM, Stewart RB, Anderson CW, Robinson BH. 2003. Nickel and cobalt phytoextraction by the hyperaccumulator *Berkheya coddii*: implications for polymetallic phytomining and phytoremediation. Int J Phytoremediation. 5(3):235-244. doi:10.1080/713779223.

Kowalska J, Stryjewska E, Bystrzejewska-Piotrowska G, Lewandowski, K, Tobiasz M, Pańdyna J, Golimowski J. 2012. Studies of plants useful in the re-cultivation of heavy metals-contaminated wasteland - A new hyperaccumulator of barium?. Pol J Environ Stud. 21(2):401-405.

Krämer U. 2010. Metal hyperaccumulation in plants. Annu Rev Plant Biol. 61:517-534. doi:10.1146/annurev-arplant-042809-112156.

Li G, Hu N, Ding D, Zheng J, Liu Y, Wang Y, Nie X. 2011. Screening of plant species for phytoremediation of uranium, thorium, barium, nickel, strontium and lead contaminated soils from a uranium mill tailings repository in South China. Bull Environ Contam Toxicol. 86:646-652. doi:10.1007/s00128-011-0291-2.

Marschner H. 2016. Marschner's Mineral Nutrition of Higher Plants. 3rd ed. San Diego (US): Academic Press.

Menezes de Sequeira E, Pinto da Silva A. 1992. Ecology of serpentinized areas of north-east Portugal. In: Roberts BA, Proctor J, editors. The ecology of areas with serpentinized rocks. Dordrecht (NE): Springer. p. 169-197.

Mišljenović T, Jovanović S, Mihailović N, Gajić B, Tomović G, Baker A, Echevarria G, Jakovljević K. 2019. Natural variation of nickel, zinc and cadmium (hyper) accumulation in facultative serpentinophytes *Noccaea kovatsii* and *N. praecox*. Plant Soil. 447:475-495. doi:10.1007/s11104-019-04402-5.

Morais I, Campos J, Favas P, Pratas J, Pita F, Prasad M. 2015. Nickel accumulation by *Alyssum serpyllifolium* subsp. *lusitanicum* (Brassicaceae) from serpentine soils of Bragança and Morais (Portugal) ultramafic massifs: plant-soil relationships and prospects for phytomining. Aust J Bot. 63(2):17-30. doi:10.1071/BT14245.

Morishita T, Nakamura K, Shibuya T, Kumagai H, Sato T, Okino K, Sato H, Nauchi R, Hara K, Takamaru R. 2015. Petrology of peridotites and related gabbroic rocks around the Kairei hydrothermal field in the Central Indian Ridge. In: Ishibashi J, Okino K, Sunamura M, editors. Subseafloor Biosphere Linked to Hydrothermal Systems. Tokyo (JA): Springer. p. 177-193.

Mota J, Garrido-Becerra J, Merlo M, Medina-Cazorla J, Sánchez-Gómez P. 2017. The edaphism: gypsum, dolomite and serpentine flora and vegetation. In: Loidi J, editors. The Vegetation of the Iberian Peninsula. Plant and Vegetation. Vol 13. Cham (GE): Springer. p. 277-354.

Oliveras V, Galán G. 2006. Petrología y mineralogía de los xenolitos mantélicos del volcán la Banya del Boc (Girona) [Petrology and mineralogy of mantle xenoliths from La Banya del Boc volcano (Girona)]. Geogaceta. 40:107-110.

Pavlova D, Karadjova I. 2013. Toxic element profiles in selected medicinal plants growing on serpentines in Bulgaria. Biol Trace Elem Res. 156:288-297. doi:10.1007/s12011-013-9848-8.

Pérez Latorre AV, Hidalgo-Triana N, Cabezudo B. 2013. Composition, ecology and conservation of the South-Iberian serpentine flora in the context of the Mediterranean basin. An Jard Bot Madr. 70(1):62-71.

Pérez Latorre AV, Navas P, Navas D, Gil Y & Cabezudo B. 1998. Datos sobre la flora y vegetación de la Serranía de Ronda (Málaga, España) [Data on the flora and vegetation of the Serranía de Ronda (Malaga, Spain)]. Acta Bot Malacit. 23:149-191. doi:10.24310/abm.v23i0.8557.

Pollard A, McCartha G, Quintela-Sabarís C, Flynn T, Sobczyk M, Smith JAC. 2021. Intraspecific variation in nickel tolerance and hyperaccumulation among serpentine and limestone populations of *Odontarrhena serpyllifolia* (Brassicaceae: Alysseae) from the Iberian Peninsula. Plants. 10(4):800. doi:10.3390/plants10040800.

Pons J, Leyva C, Rodríguez G, Ramírez M. 2000. Características físico-químicas de las dunitas serpentinizadas de la región de Moa-Baracoa (Zonas Amores y Miraflores) [Physico-chemical characteristics of the serpentine dunites of the Moa-Baracoa region (Amores and Miraflores Zones)]. Min Geolog. 17(3-4):95-99.

Prasad MNV, Freitas HMO. 1999. Feasible biotechnological and bioremediation strategies for serpentine soils and mine spoils. Electron J Biotechnol. 2:36-50. doi:10.4067/S0717-34581999000100003.

Rajakaruna N. 2004. The edaphic factor in the origin of species. Int Geol Rev. 46(5):471-478. doi:10.2747/0020-6814.46.5.471.

Rivas-Goday S. 1973. Plantas serpentinícolas y dolomitícolas del sur de España [Serpentine and dolomitic plants of southern Spain]. Bol Soc Brot. 47(2):161-178.

Rivas-Martínez S, Díaz ET, Fernández-González F, Izco J, Loidi J, Lousä M, et al. 2002. Vascular plant communities of Spain and Portugal. Addenda to the syntaxonomical checklist of 2001. Itinera Geobot. 15:5-922. Madrid (SP): Centro de Investigaciones Fitosociológicas; [accessed 2021 Aug 30]. https://www.globalbioclimatics.org/book/addenda/addenda2_22.htm.

Rodríguez N, Menéndez N, Tornero J, Amils R, de la Fuente V. 2005. Internal iron biomineralization in *Imperata cylindrica*, a perennial grass: chemical composition, speciation and plant localization. New Phytol. 165(3):781-789. doi:10.1111/j.1469-8137.2004.01264.x.

Romero-Freire A, Olmedo-Cobo J, Gómez-Zotano J. 2018. Elemental concentration in serpentinitic soils over ultramafic bedrock in Sierra Bermeja (Southern Spain). Minerals. 8(10):447. doi:10.3390/min8100447.

Rowell D. 2014. Soil science: methods & applications. London (UK): Routledge.

Rue M, Paul A, Echevarria G, van der Ent A, Simmonot M, Morel JL. 2020. Uptake, translocation and accumulation of nickel and cobalt in *Berkheya coddii*, a ‘metal crop’ from South Africa. Metallomics. 12(8): 1278-1289. doi:10.1039/d0mt00099j.

Rufo L, Rodríguez N, de la Fuente V. 2005. Análisis comparado de metales en suelos y plantas de la Sierra Bermeja [Comparative analysis of metals in soils and plants of the Sierra Bermeja]. In: Jiménez-Ballesta R, Álvarez González AM, editors. II Simposio Nacional de Control de la Degradación de Suelos: Comunicaciones; 2005 Jul 6-8. Madrid (SP): Universidad Autónoma de Madrid. p. 197-201.

Shabala S. 2013. Learning from halophytes: physiological basis and strategies to improve abiotic stress tolerance in crops. Ann Bot. 112(7):1209-1221. doi:10.1093/aob/mct205.

Sheoran V, Sheoran AS, Poonia P. 2010. Role of hyperaccumulators in phytoextraction of metals from contaminated mining sites: a review. Crit Rev Environ Sci Technol. 41:168-214. doi:10.1080/10643380902718418.

Španiel S, Kempa M, Salmerón-Sánchez E, Fuertes-Aguilar J, Mota J, Al-Shehbaz I, German D, Olšavská K, Šingliarova B, Zozomová-Lihová J, et al. 2015. AlyBase: database of names, chromosome numbers, and ploidy levels of Alysseae (Brassicaceae), with a new generic concept of the tribe. Plant Syst Evol. 301:2463-2491. doi:10.1007/s00606-015-1257-3.

Sterckeman T, Cazes Y, Gonneau C, Sirguey C. 2017. Phenotyping 60 populations of *Noccaea caerulescens* provides a broader knowledge of variation in traits of interest for phytoextraction. Plant Soil. 418:523-540. doi:10.1007/s11104-017-3311-0.

van der Ent A, Baker A, Reeves R, Chaney R, Anderson C, Meech J, Erskine P, Simonnot M, Vaughan J, Morel J, et al. 2015. Agromining: farming for metals in the future?. Environ Sci Technol. 49(8):4773-4780. doi:10.1021/es506031u.

van der Ent A, Baker A, Reeves R, Pollard A, Schat H. 2013. Hyperaccumulators of metal and metalloid trace elements: facts and fiction. Plant Soil. 362:319-334. doi:10.1007/s11104-012-1287-3.

van der Ent A, Echevarria G, Pollard A, Erskine P. 2019. X-ray fluorescence ionomics of herbarium collections. Sci Rep. 9:4746. doi:10.1038/s41598-019-40050-6.

Verbruggen N, Hermans C, Schat H. 2009. Molecular mechanisms of metal hyperaccumulation in plants. New Phytol. 181(4):759-776. doi:10.1111/j.1469-8137.2008.02748.x.

Vithanage M, Rajapaksha AU, Oze C, Rajakaruna N, Dissanayake CB. 2014. Metal release from serpentine soils in Sri Lanka. Environ Monit Assess. 186:3415-3429. doi:10.1007/s10661-014-3626-8.

Wang X, Shan T, Pang S. 2018. Phytoremediation potential of *Saccharina japonica* and *Sargassum horneri* (Phaeophyceae): biosorption study of strontium. Bull Environ Contam Toxicol. 101:501-505. doi:10.1007/s00128-018-2435-0.

Table 1. Analysis of variance (Kruskal-Wallis test) of the soil and the leaves parameters between the different petrographic entities. *P* values <0.05 are marked in bold.

Variable	**p** Soil	**p** Leaves
Fe	**0.02**	0.07
Mg	**0.02**	0.13
Si	0.07	0.07
Ni	0.207	0.34
Cr	0.109	0.41
Co	0.149	0.77
Sr	**0.03**	0.17
Mn	0.31	0.21
Cu	0.40	0.05
Zn	0.27	0.22
Ba	**0.04**	0.34

Table 2. Bioaccumulation factors (BAF) for the metals analysed at each type of sampling site. (Bd) dunites, (Bh) harzburgite-pyroxenic dunite, (Bl) harzburgite-lherzolite, (Bp) pyroxenite and (Ms) serpentinites. The highest BAF values for Ni and Sr are underlined.

	Fe	Mg	Si	Ni	Cr	Co	Sr	Mn	Cu	Zn	Ba
Bd	0.01	0.07	0.02	**2.64**	0.01	0.22	**10.54**	0.06	0.05	0.18	0.65
Bh	<0.01	0.07	0.01	**2.49**	<0.01	0.21	**4.94**	0.06	0.07	0.14	0.36
Bl	0.01	0.09	0.02	**3.47**	0.01	0.20	**4.42**	0.06	0.07	0.11	0.33

Bp	0.01	0.09	0.02	**3.06**	<0.01	0.17	**12.92**	0.07	0.08	0.34	0.61
Ms	<0.01	0.07	0.01	**1.92**	<0.01	0.17	**3.71**	0.04	0.04	0.11	0.22

Values >1 are in bold, the highest value for Ni and Sr are also underlined

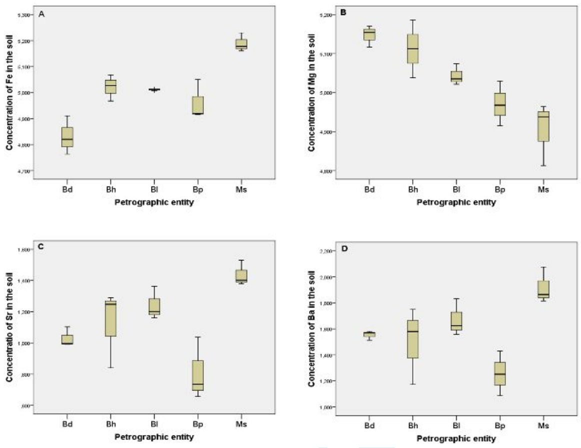

Figure 1. Boxplot for concentrations of (A) Fe in the soil, (B) Mg in the soil, (C) Sr in the soil and (D) Ba the in soil across the petrographic entities. From left to right, the dunites (Bd), harzburgite-pyroxenic dunite (Bh), harzburgite-lherzolite (Bl), pyroxene (Bp) and serpentinites (Ms).

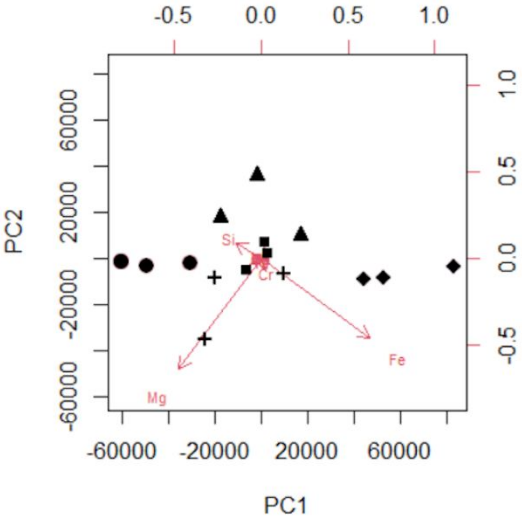

Figure 2. PCA biplot of soil elements. Samples collected on (□) dunites unit (Bd), **(+)** harzburgite-pyroxenic dunite unit (Bh), (⍰) harzburgite-lherzolite unit (Bl), (▲) pyroxenite unit (Bp) and (◆) serpentinites unit (Ms).

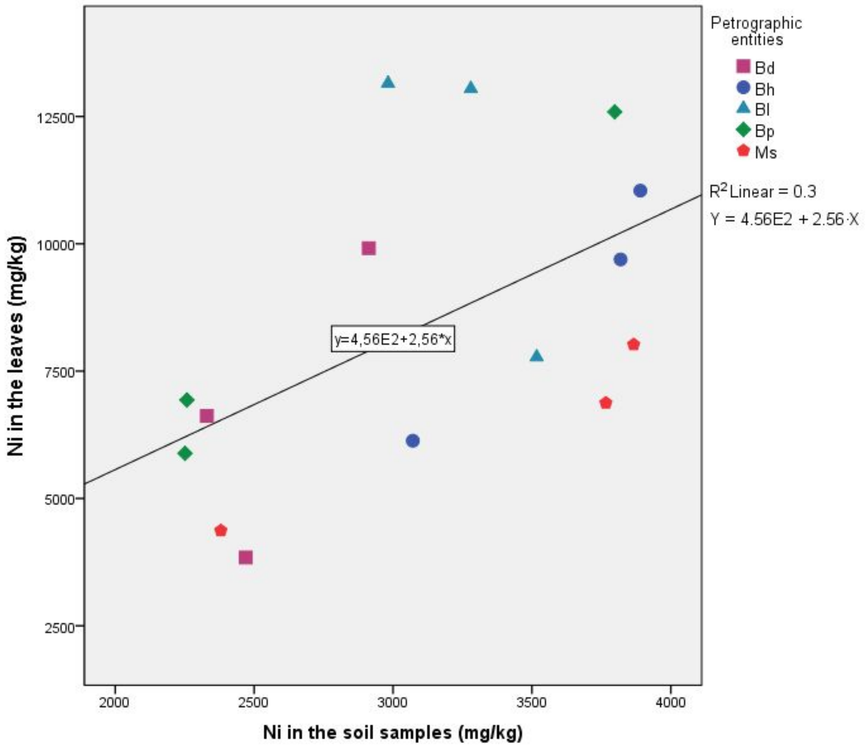

Figure 3. Linear regression of the concentration of Ni in leaf samples and the concentration of Ni in soil samples. (Bd) dunites, (Bh) harzburgite-pyroxenic dunite, (Bl) harzburgite-lherzolite, (Bp) pyroxenite and (Ms) serpentinites.

Supporting information

Figure S1. Location of ultramafic massifs of Southern Iberian Peninsula (Malaga). Own elaboration according to the National Geological Map at 1:50000 scale (MAGNA50) of the Geological and Mining Institute of Spain and the coverage available in DERA (Junta de Andalucia 2020).

Junta de Andalucía (2020) Datos Espaciales de Referencia de Andalucía (DERA). In: Instituto de Estadística y Cartografía de Andalucía. Available via online.

https://www.juntadeandalucia.es/institutodeestadisticaycartografia/DERA/. Accessed 30 Aug 2021

Figure S2. Georeferenced geological map of the study areas elaborated according to the previous existent National Geological Map at 1:50000 scale (MAGNA50) and location of studied sites. Studied massifs with petrographic entities: A: Sierra Bermeja (Bd, on dunites; Bp, on pyroxenite; Bh, on harzburgite-pyroxenic dunite and Bl, on harzburgite-lherzolite) and B: Sierra de Mijas (Ms, on serpentinites). (NUR) Non-ultramafic rocks, (D) dunites, (H-Pd) harzburgite-pyroxenic dunite, (H-L) harzburgite-lherzolite, (UP) undifferentiated peridotite, (P) pyroxenite, (S) serpentinites. Own elaboration.

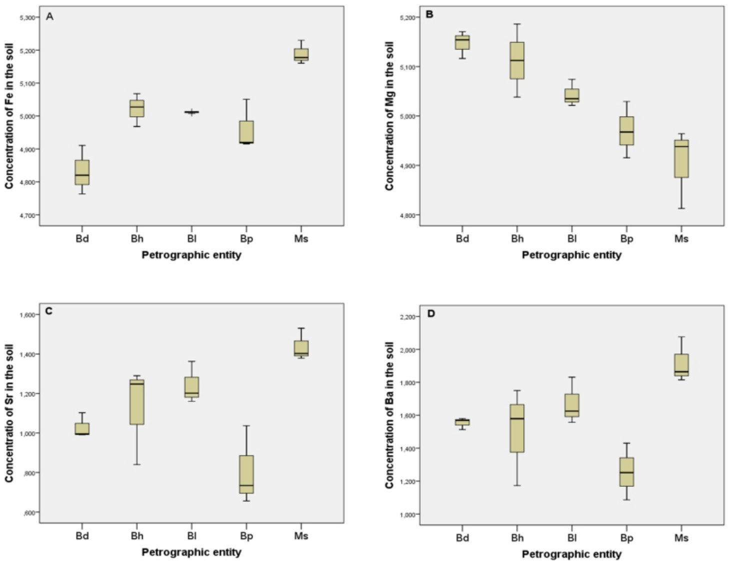

Boxplot for concentrations of (A) Fe in the soil, (B) Mg in the soil, (C) Sr in the soil and (D) Ba the in soil across the petrographic entities. From left to right, the dunites (Bd), harzburgite-pyroxenic dunite (Bh), harzburgite-lherzolite (Bl), pyroxene (Bp) and serpentinites (Ms).

338x190mm (300 x 300 DPI)

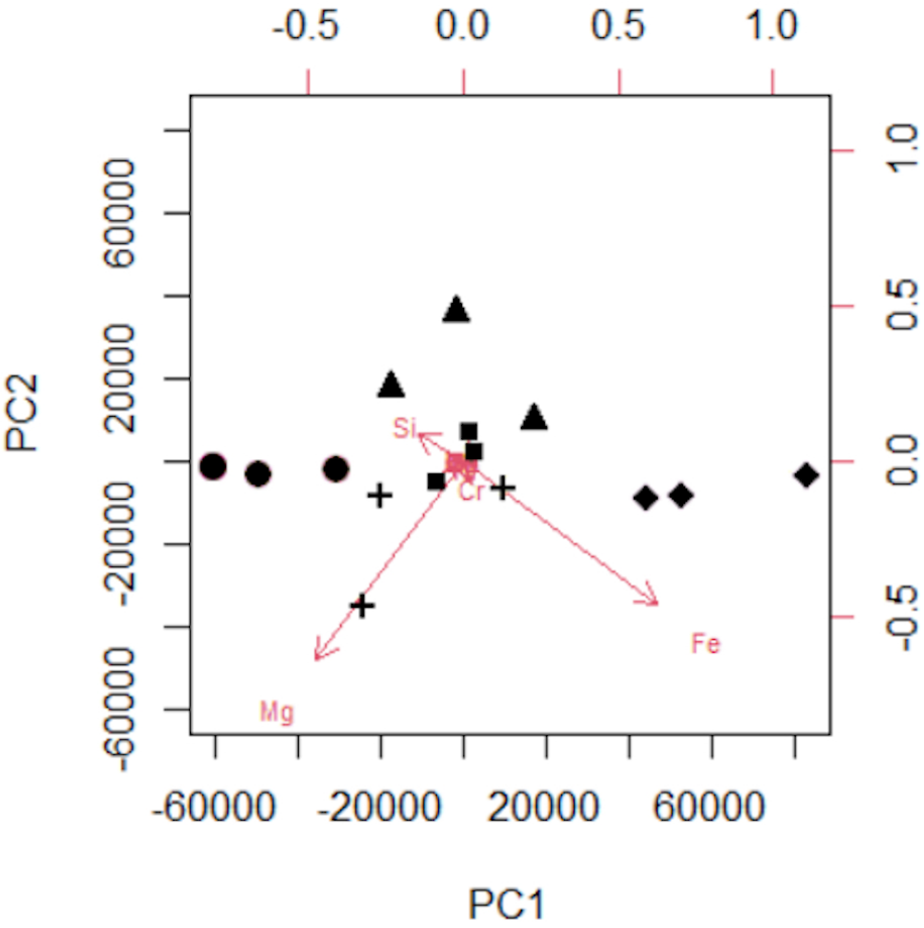

PCA biplot of soil elements. Samples collected on (☐) dunites unit (Bd), (+) harzburgite-pyroxenic dunite unit (Bh), (☐) harzburgite-lherzolite unit (Bl), (▲) pyroxenite unit (Bp) and (◆) serpentinites unit (Ms).

83x82mm (300 x 300 DPI)

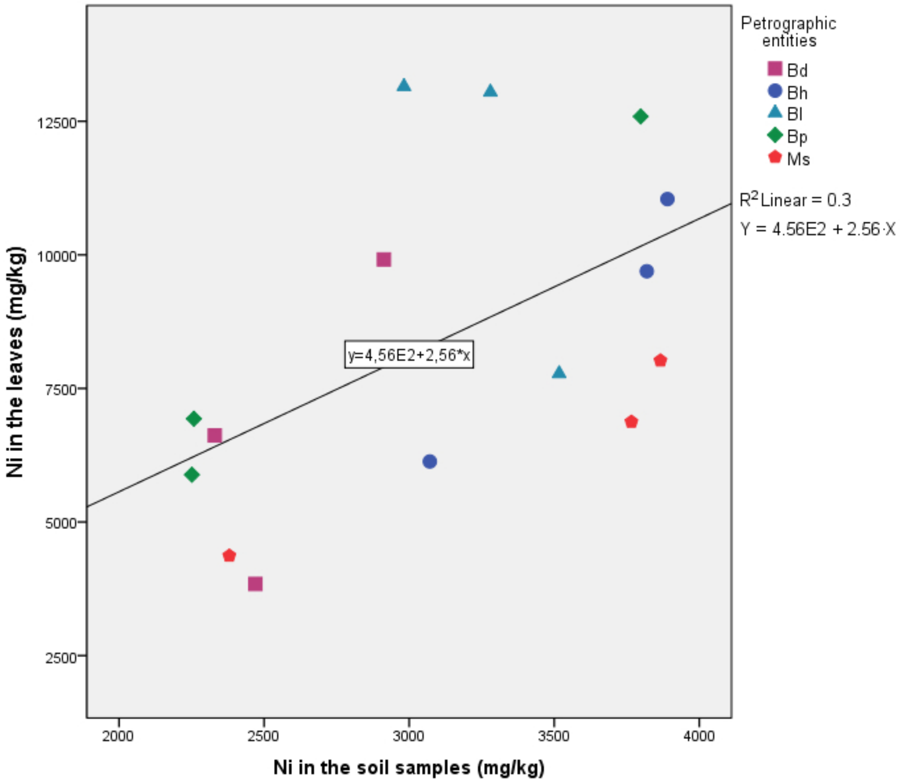

Figure 3. Linear regression of the concentration of Ni in leaf samples and the concentration of Ni in soil samples. (Bd) dunites, (Bh) harzburgite-pyroxenic dunite, (Bl) harzburgite-lherzolite, (Bp) pyroxenite and (Ms) serpentinites.

267x213mm (72 x 72 DPI)

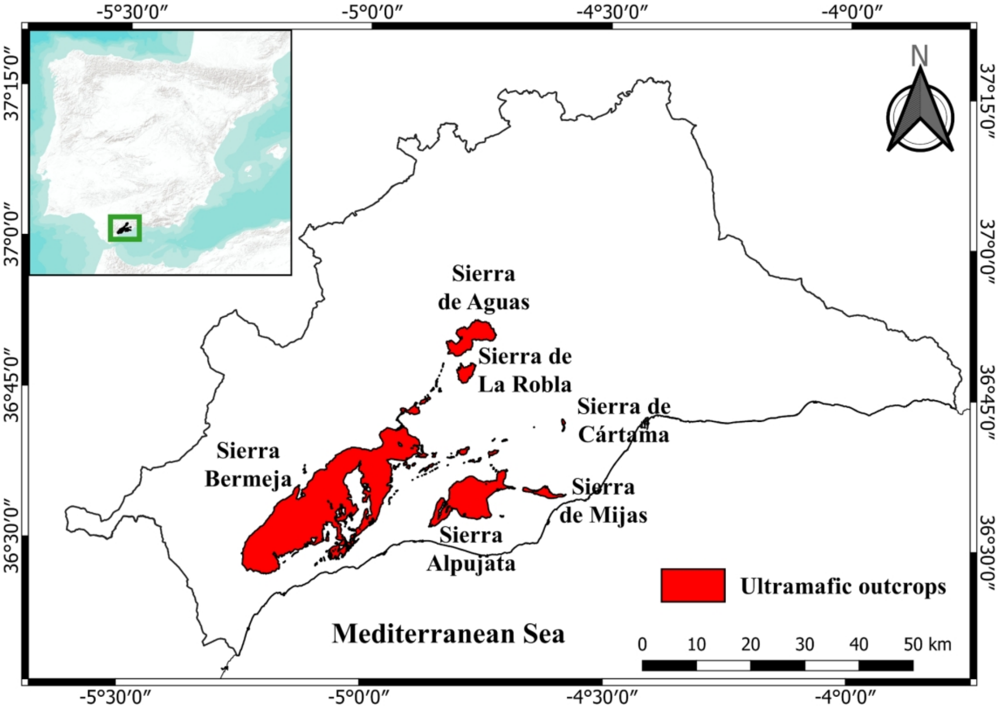

173x123mm (300 x 300 DPI)

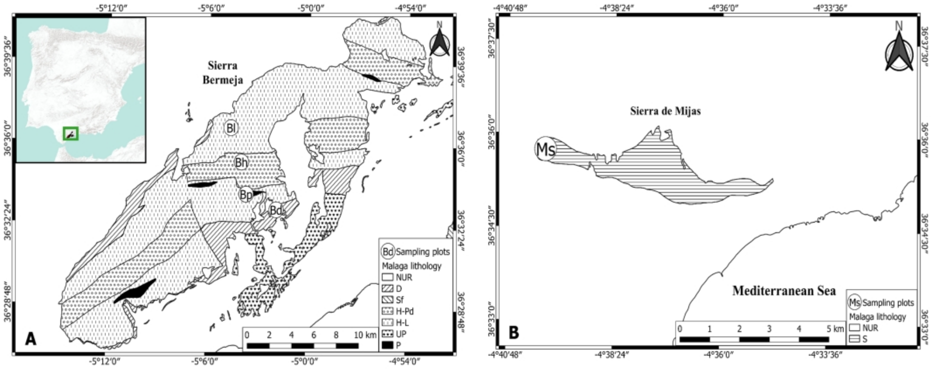

338x190mm (300 x 300 DPI)

Table S1. Characterization of the studied points. The petrographic entities at each sampling site were determined according to the appropriate geological maps (MAGNA50). Textural classes follow USDA classification (Rowell 2014). Bioclimatic parameters for each location were extracted from Rivas Martínez et al. (2002) and Vegetation type from Gálvez-Villamuela et al. (2021) and Pérez Latorre et al. (1998, 2013).

Sampling site code	**Coordinates (DMS)**	**Altitude (masl)**	**Massif**	**Petrographic entities: bedrock types**	**Soil type (USDA)**	**Bioclimatic unit: Thermotype (main annual T)**	**Bioclimatic unit: Ombrotype (main annual rainfall)**	**Vegetation**
Bd	36°33´15.38´´/ -5°2´7.77´´	509	S. Bermeja	Dunites	Entisol	Thermomediterranean (17-18ºC)	Subhumid (600-800 mm)	Scrubland: *Halimio atripicifolii-Digitaletum laciniatae*

Bh	36°35´13.64´´/ -5°4´1.93´´	842	S. Bermeja	Harzburgite-pyroxenic dunite	Entisol	Mesomediterranean (15-16ºC)	Humid (1000-1300 mm)	Pine forest: *Pino acutisquamae-Quercetum cocciferae*
Bl	36°36´49.92´´/ -5°4´30.00´´	1044	S. Bermeja	Harzburgite-lherzolite	Entisol	Mesomediterranean (15-16ºC)	Humid (1000-1300 mm)	Scrubland: *Halimio atripicifolii-Digitaletum laciniatae*
Bp	36°33´46.90´´/ -5°3´34.08´´	655	S. Bermeja	Pyroxenite	Entisol	Thermomediterranean (17-18ºC)	Subhumid (600-800 mm)	Pine forest: *Pino acutisquamae-Quercetum cocciferae*

Ms	36°35´47.15´´/ -4°40´5.61´´	367	S. de Mijas	Serpentinites	Entisol	Thermomediterranean (17-18ºC)	Subhumid (600-800 mm)	Graminoid perennial pasture: *Scorzonero baeticae-Macrochloetum tenacissimae*

Table S2. Descriptive statistics of leaves (l) and of soil (s) parameters analysed of *A. serpyllifolium* subsp. *malacitanum*. All values are given in mg·kg^{-1}. SD = standard deviation; Min = minimum, Max = maximum; CV = coefficient of variation. Sampling sites: (Bd) dunites, (Bh) harzburgite-pyroxenic dunite, (Bl) harzburgite-lherzolite, (Bp) pyroxenite and (Ms) serpentinites.

Parameters	**Sampling site**	**Mean ± SD**	**Minimum**	**Maximum**	**CV (%)**
Fe_l	Bd	743.67 ± 414	330	1158	55.7
Fe_s	Bd	68500 ± 11883.18	58000	81400	17.3
Fe_l	Bh	240 ± 78.31	152	302	32.6
Fe_s	Bh	105433.33 ± 12035.5	92900	116900	11.4
Fe_l	Bl	**987** ± 962.31	414	2098	97.5
Fe_s	Bl	102596.67 ± 799.4	101690	103200	0.8
Fe_l	Bp	598.33 ± 374.01	318	1023	62.5
Fe_s	Bp	92566.67 ± 17179.74	82300	112400	18.6
Fe_l	Ms	294.67 ± 93.61	191	373	31.8
Fe_s	Ms	**155006.67 ± 13157.57**	144710	169830	8.5
Mean±SD		52696.701±58843.27			33.67
Mean±SD l		572.734 ± 312.06			
Mean±SD s		104820.668 ± 31596.31			
Mg_l	Bd	**10264** ± 1897.72	8574	12317	18.5
Mg_s	Bd	**140466.67** ± 8894.01	130700	148100	6.3
Mg_l	Bh	9436 ± 2922.63	6262	12016	30.9
Mg_s	Bh	130733.33 ± 22175.74	109200	153500	17
Mg_l	Bl	9927.33 ± 2336.89	7945	12504	23.5
Mg_s	Bl	110693.33 ± 7045.72	105080	118600	6.4
Mg_l	Bp	8645 ± 1652.71	6957	10260	19.1

Mg_s	Bp	94033.33 ± 12396.1	82300	107000	13.2
Mg_l	Ms	5782 ± 252.63	5553	6053	4.4
Mg_s	Ms	81253.33 ± 14336.24	64990	92060	17.6
Mean±SD		60123.432 ± 56541.34			15.69
Mean±SD l		8810.866 ± 1799.33			
Mean±SD s		111435.998 ± 24645.31			
Si_l	Bd	**3496.67** ± 190.14	3285	3653	5.4
Si_s	Bd	161533.33 ± 4219.4	157100	165500	2.6
Si_l	Bh	1854.33 ± 522.04	1494	2453	28.2
Si_s	Bh	159766.67 ± 3780.65	155500	162700	2.4
Si_l	Bl	2837.33 ± 1503.79	1925	4573	53
Si_s	Bl	153010 ± 7300.02	145700	160300	4.8
Si_l	Bp	2764.33 ± 898.65	2244	3802	32.5
Si_s	Bp	**162633.33** ± 7102.35	154700	168400	4.4
Si_l	Ms	1500.33 ± 238.89	1354	1776	15.9
Si_s	Ms	144433.33 ± 9663.61	133650	152310	6.7
Mean±SD		79382.965 ± 81211.73			15.59
Mean±SD l		2490.598 ± 805.11			
Mean±SD s		156275.332 ± 7601.90			
Ni_l	Bd	6791.67 ± 3040.14	3841	9914	44.8
Ni_s	Bd	2571 ± 304.34	2330	2913	11.8
Ni_l	Bh	8956.67 ± 2537.65	6132	11044	28.3
Ni_s	Bh	**3593.33** ± 453.75	3071	3890	12.6
Ni_l	Bl	**11324.33** ± 3073.38	7776	13150	27.1
Ni_s	Bl	3259.67 ± 268.08	2982	3517	8.2
Ni_l	Bp	8469.67 ± 3606.66	5885	12590	42.6

Ni_s	Bp	2769 ± 891.15	2251	3798	32.2
Ni_l	Ms	6422.33 ± 1868.28	4369	8022	29.1
Ni_s	Ms	3337.33 ± 830.58	2380	3866	24.9
Mean±SD		5749.5 ± 3090.41			26.16
Mean±SD l		8392.934 ± 1959.85			
Mean±SD s		3106.066 ± 422.61			
Cr_l	Bd	19.55 ± 15.66	4.94	36.08	80.1
Cr_s	Bd	3446 ± 1055.54	2455	4556	30.6
Cr_l	Bh	4.56 ± 3.33	2.33	8.39	72.9
Cr_s	Bh	**8089** ± 3960.92	3723	11452	49
Cr_l	Bl	**37.18** ± 51.25	7.4	96.36	137.8
Cr_s	Bl	5871 ± 3304.45	3867	9685	56.3
Cr_l	Bp	8.16 ± 3.99	4.24	12.22	48.9
Cr_s	Bp	2617.67 ± 1136.13	1860	3924	43.4
Cr_l	Ms	6.35 ± 3.66	3.25	10.38	57.2
Cr_s	Ms	8013.67 ± 2938.39	5118	10993	36.7
Mean±SD		2811.314 ± 3396.30			61.29
Mean±SD l		15.16 ± 13.63			
Mean±SD s		5607.468 ± 2531.21			
Co_l	Bd	42.32 ± 18.48	29.26	63.46	43.7
Co_s	Bd	196.19 ± 18.65	177.13	214.39	9.5
Co_l	Bh	**47.93** ± 12.12	38.29	61.54	25.3
Co_s	Bh	232.7 ± 12.51	225.32	247.14	5.4
Co_l	Bl	45.09 ± 23.3	28.69	71.76	51.7
Co_s	Bl	223.94 ± 11.73	216.21	237.44	5.2
Co_l	Bp	34.67 ± 9.69	25.79	45	27.9
Co_s	Bp	206.8 ± 20.47	184.58	224.89	9.9
Co_l	Ms	43.74 ± 11.43	30.55	50.39	26.1
Co_s	Ms	**261.98** ± 65.37	188.89	314.86	25
Mean±SD		133.536± 97.24			22.97

Mean±SD l		42.75 ± 4.97			
Mean±SD s		224.322 ± 25.43			
Sr_l	Bd	**113.62** ± 34.84	88.9	153.46	30.7
Sr_s	Bd	10.78 ± 1.63	9.8	12.66	15.1
Sr_l	Bh	72.6 ± 14.1	63.1	88.79	19.4
Sr_s	Bh	14.7 ± 6.8	6.92	19.49	46.2
Sr_l	Bl	78.67 ± 27.75	46.8	97.48	35.3
Sr_s	Bl	17.8 ± 4.59	14.46	23.04	25.8
Sr_l	Bp	89.75 ± 20.03	66.79	103.69	22.3
Sr_s	Bp	6.95 ± 3.44	4.53	10.89	49.5
Sr_l	Ms	102.7 ± 10	91.18	109.17	9.7
Sr_s	Ms	**27.69** ± 5.4	23.93	33.88	19.5
Mean±SD		53.526±41.88			27.35
Mean±SD l		91.468 ± 16.87			
Mean±SD s		15.584 ± 7.90			
Mn_l	Bd	135.49 ± 21.44	112.35	154.68	15.8
Mn_s	Bd	2087 ± 68.02	2040	2165	1.8
Mn_l	Bh	122 ± 24.98	98.99	148.57	20.5
Mn_s	Bh	2087.67 ± 195.24	1969	2313	9.4
Mn_l	Bl	125.88 ± 25.56	106.32	154.8	20.3
Mn_s	Bl	2205.33 ± 105.64	2103	2314	4.8
Mn_l	Bp	**151** ± 35.23	72.72	113.2	23.3
Mn_s	Bp	2042 ± 135.63	1928	2192	6.6
Mn_l	Ms	86.33 ± 23.27	72.72	113.2	27
Mn_s	Ms	**2428.67** ± 481.82	2050	2971	19.8
Mean±SD		1147.137 ±1083.50			14,93
Mean±SD l		124.14 ± 23.91			
Mean±SD s		2170.134 ± 156.69			
Cu_l	Bd	3.29 ± 0.78	2.55	4.1	23.7
Cu_s	Bd	**64.47** ± 36	35.97	104.93	55.8

Cu_l	Bh	2.05 ± 0.29	1.76	2.33	14
Cu_s	Bh	29.17 ± 2.13	26.73	30.65	7.3
Cu_l	Bl	2.28 ± 0.07	2.21	2.35	3
Cu_s	Bl	31.39 ± 8.72	23.66	40.84	27.8
Cu_l	Bp	**3.41** ± 2.46	1.88	6.24	72.1
Cu_s	Bp	44.6 ± 22.42	25.58	69.31	50.3
Cu_l	Ms	1.59 ± 0,2	1.42	1.81	12.6
Cu_s	Ms	36.15 ± 12.73	22.61	47.87	35.2
Mean±SD		21.84 ± 24.49			30.18
Mean±SD l		2.524 ± 0.80			
Mean±SD s		41.156 ± 14.31			
Zn_l	Bd	20.84 ± 1.61	19.86	22.69	7.7
Zn_s	Bd	113.48 ± 13.79	104.3	129.34	12.2
Zn_l	Bh	17.06 ± 5.81	11.74	23.26	34.1
Zn_s	Bh	119.51 ± 32.15	82.39	138.34	26.9
Zn_l	Bl	10.9 ± 0.72	10.22	11.66	6.6
Zn_s	Bl	97.44 ± 22.76	79.12	122.92	23.4
Zn_l	Bp	**44.08** ± 43.73	10.89	93.63	99.2
Zn_s	Bp	128.71 ± 52.42	88.05	187.88	40.7
Zn_l	Ms	15.64 ± 6.48	8.58	21.32	41.4
Zn_s	Ms	**143.89** ± 13.16	129.54	155.39	9.1
Mean±SD		71.155 ± 54.09			30.13
Mean±SD l		21.704 ± 13.00			
Mean±SD s		120.606 ± 17.29			
Ba_l	Bd	**23.36** ± 12.49	10.45	35.38	53.5
Ba_s	Bd	35.84 ± 2.89	32.55	38	8.1
Ba_l	Bh	13.01 ± 9.32	6.94	23.74	71.6
Ba_s	Bh	36.34 ± 20.72	14.88	56.22	57
Ba_l	Bl	16.05 ± 6,91	8.44	21.94	43.1
Ba_s	Bl	48.7 ± 16.84	36.06	67.81	34.6

Ba_l	Bp	11.53 ± 2.78	8.4	13.71	24.1
Ba_s	Bp	19 ± 7.45	12.2	26.95	39.2
Ba_l	Ms	18.72 ± 2.65	16.32	21.57	14.2
Ba_s	Ms	**85.87** ± 29.03	65.37	119.09	33.8
Mean±SD		30.842 ± 22.74			37.92
Mean±SD l		16.53 ± 4.72			
Mean±SD s		45.15 ± 25.09			

Highest values of soil and leaves parameters are in bold, lowest values are underlined.

Table S3. Coefficient values of variables for the two principal components of PCA.

Variable	**PC1**	**PC2**
Fe	0.7825697	-0.5783904
Mg	-0.5939607	-0.8027945
Si	-0.1822621	0.1131823
Ni	0.0082289	-0.0199523
Cr	0.0385986	-0.0881818
Co	0.0006727	-0.0006936
Sr	0.0001570	-0.0001367
Mn	0.0041579	-0.0000788
Cu	-0.0001556	0.0004063
Zn	0.0003115	0.0006444
Ba	0.0005343	-0.0003916

Table S4. Correlations between element concentrations in the leaves from the studied populations. Significant pairwise element correlations. N = 12 for Sierra Bermeja Massif and N = 3 for Sierra de Mijas Massif.

Element in leaves	Correlation with other elements in leaves
Fe	Si(+)**, Cr(+)**, Mn(+)*, Cu(+)*
Mg	Si(+)**, Mn(+)**, Cu (+)*
Si	Fe(+)**, Mg(+)**, Cr(+)*, Mn(+)**, Cu(+)**
Ni	-
Cr	Fe(+)**, Si(+)*
Co	-
Sr	-
Mn	Fe(+)*, Mg(+)**, Si(+)**
Cu	Fe(+)*, Mg(+)*, Si(+)**
Zn	-
Ba	-

Significance: * ($p < 0.05$); ** ($p < 0.01$).

Table S5. Correlations between element concentrations in the leaves (l) and their soils (s) from the studied populations. N= 12 for Sierra Bermeja Massif and N= 3 for Sierra de Mijas Massif.

Element	Significant pairwise element correlations
Fe	Fe_l-Cu_s (+)*, Fe_s-Mg_l (-)*, Fe_s-Si_l (-)**, Fe_s-Cu_l(-)**
Mg	Mg_l-Fe_s(-)*
Si	Si_l-Fe_s(-)**, Si_s-Cu_l(+)*, Si_s-Zn_l(+)*
Ni	Ni_l-Ni_s(+)*, Ni_s-Co_l(+)**
Cr	Cr_l-Cu_s(+)*
Co	Co_l-Ni_s(+)**, Co_s-Cu_l(-)**, Co_s-Zn_l(-)*
Sr	Sr_s-Cu_l(-)*

Mn	-
Cu	Cu_l-Fe_s(-)**, Cu_l-Si_s (+)*, Cu_l-Co_s (-)**, Cu_l-Sr_s(-)*, Cu_s-Fe_l(+)*, Cu_s-Cr_l(+)*
Zn	Zn_l-Si_s(+)*, Zn_l-Co_s(-)*
Ba	-

Significance: * ($p < 0.05$); ** ($p < 0.01$).